Article

Characterization of Inhibitory Effectiveness in Hyperpolarization-Activated Cation Currents by a Group of *ent*-Kaurane-Type Diterpenoids from *Croton tonkinensis*

Ping-Chung Kuo [1] , **Yen-Chin Liu** [2] , **Yi-Ching Lo** [3] **and Sheng-Nan Wu** [4,5,*]

[1] School of Pharmacy, National Cheng Kung University Medical College, Tainan 70101, Taiwan; z10502016@email.ncku.edu.tw
[2] Department of Anesthesiology, National Cheng Kung University Hospital, College of Medicine, National Cheng Kung University, Tainan 70101, Taiwan; inp1965@mail.ncku.edu.tw
[3] Department of Pharmacology, Kaohsiung Medical University, Kaohsiung 80708, Taiwan; yichlo@kmu.edu.tw
[4] Department of Physiology, National Cheng Kung University Medical College, Tainan 70101, Taiwan
[5] Institute of Basic Medical Sciences, National Cheng Kung University Medical College, Tainan 70101, Taiwan
[*] Correspondence: snwu@mail.ncku.edu.tw; Tel.: +886-6-2353535-5334; Fax: 886-6-2362780

check for updates

Abstract: Croton is an extensive flowering plant genus in the spurge family, Euphorbiaceae. Three croton compounds with the common *ent*-kaurane skeleton have been purified from *Croton tonkinensis*. Methods: We examined any modifications of croton components (i.e., croton-01 [*ent*-18-acetoxy-7α-hydroxykaur-16-en-15-one], croton-02 [*ent*-7α,14β-dihydroxykaur-16-en-15-one] and croton-03 [*ent*-1β-acetoxy-7α,14β-dihydroxykaur-16-en-15-one] on either hyperpolarization-activated cation current (I_h) or *erg*-mediated K^+ current identified in pituitary tumor (GH$_3$) cells and in rat insulin-secreting (INS-1) cells via patch-clamp methods. Results: Addition of croton-01, croton-02, or croton-03 effectively and differentially depressed I_h amplitude. Croton-03 (3 μM) shifted the activation curve of I_h to a more negative potential by approximately 11 mV. The voltage-dependent hysteresis of I_h was also diminished by croton-03 administration. Croton-03-induced depression of I_h could not be attenuated by SQ-22536 (10 μM), an inhibitor of adenylate cyclase, but indeed reversed by oxaliplatin (10 μM). The I_h in INS-1 cells was also depressed effectively by croton-03. Conclusion: Our study highlights the evidence that these *ent*-kaurane diterpenoids might conceivably perturb these ionic currents through which they have high influence on the functional activities of endocrine or neuroendocrine cells.

Keywords: croton; pituitary cell; pancreatic β-cell; hyperpolarization-activated cation current; *erg*-mediated K^+ current; membrane potential

1. Introduction

The genus *croton* (Euphorbiaceae) includes about 300 species that are widely distributed throughout tropical regions. *C. tonkinensis* Gagnep. (Euphorbiaceae), known as *Kho sam cho la* in Vietnamese, is a tropical shrub native to northern Vietnam and has been used in Vietnam for the treatment of various types of disorders [1]. Previous phytochemical investigations have shown that *C. tonkinensis* is a rich source of diterpenoids [1]. Anti-inflammatory and cancer chemopreventive activities of *C. tonkinensis* extracts have been recently reported. Those effects are thought to be linked to their ability to depress the transcription nuclear factor κB [1].

Previous studies have demonstrated that intravenous injection with the essential oil of *C. zehntneri* or *nepetaefolius* could induce rapid and dose-dependent hypotension and bradycardia [2–4].

The essential oil of *C. nepetaefolius* was reported to reverse histamine-induced firing in guinea-pig celiac ganglion [5]. The diterpene isolated from *C. argyrophylloides* was demonstrated to exert antispasmodic effects in airway smooth muscle [6].

Earlier reports have shown that the compounds purified from croton could modulate different types of ion channels. For example, either crofelemer or SP-300, a purified proanthocyanidine oligomer extracted from the South American medicinal plant *C. lechleri* (dragon's blood), has been demonstrated to depress Cl⁻ currents in colonic epithelial cells [7,8]. The diterpene isolated from *C. argyrophylloides* could block voltage-gated Ca^{2+} channels in airway smooth muscle cells [6].

Hyperpolarization-activated cation current (I_h) has been recognized as a key determinant of repetitive electrical activity present in heart cells and in a variety of central neurons, and neuroendocrine or endocrine cells [9–17]. This current with the slow activation kinetics is a mixed inward Na^+/K^+ current which is sensitive to block by CsCl, ivabradine or zatebradine [18,19], and the increase in this current magnitude can result in depolarizing membrane potential to threshold required for the generation of action potential (AP), thereby influencing pacemaker activity and impulse propagation [10,13,16,20,21]. Correspondingly, the slow kinetics of I_h in response to long-step membrane hyperpolarization can also produce long-lasting activity-dependent changes in the excitability of electrically excitable cells [17]. It has been demonstrated to be carried by the channels encoded by a family of the hyperpolarization-activated cyclic nucleotide-gated (HCN) genes, which belongs to the superfamily of voltage-gated K^+ channels and cyclic nucleotide-gated channels [10]. However, whether or how croton or other *ent*-kaurane-type diterpenoids can interact with these HCN channels to modify the amplitude and gating of I_h as well as to perturb membrane potential has thus far remained unexplored.

Therefore, the objective of this work was to investigate whether the fractions purified from *C. tonkinensis*, namely croton-01 (*ent*-18-acetoxy-7α-hydroxykaur-16-en-15-one), croton-02 (*ent*-7α,14β-dihydroxykaur-16-en15-one) and croton-03 (*ent*-1β-acetoxy-7α,14β-dihydroxykaur-16-en-15-one), could exert any perturbations on the amplitude and gating of I_h in pituitary GH₃ cells and in INS-1 insulin-secreting cells. Of interest, findings from the present results provide the evidence to unravel that these compounds can effectively interact with the HCN channel to inhibit I_h in a concentration-, time-, and state-dependent manner. Due to croton-03's high potency, the present study might be important in evaluating the in vivo mechanisms through which croton-03 or other *ent*-kaurane-type diterpenoids produce cellular functions (e.g., antinociceptive action) [22,23].

2. Results

2.1. Effects of Croton-03 and Other ent-Kaurane Diterpenoids on Hyperpolarization-Activated Cation Current (I_h) Identified in Pituitary GH₃ Cells

In an initial stage of experiments, the modifications of I_h caused by croton-03 were evaluated in GH₃ cells which were immersed in Ca^{2+}-free Tyrode's solution, and the recording pipette used was filled with K^+-containing solution. As the whole-cell current recordings were firmly established, we maintained the examined cells at the level of −40 mV, and a long-lasting membrane hyperpolarization to −110 mV was thereafter applied. Under this experimental protocol, a slowly activating current elicited by sustained hyperpolarization was readily evoked and has hence been referred as an I_h [14,18,24]. Notably, as cells were exposed to croton-03, the amplitudes of I_h by maintained hyperpolarization was progressively diminished together with a considerable slowing in activation time course of the current (Figure 1A). For example, cell exposure to 3 μM croton-03 decreased current amplitude at the end of hyperpolarizing pulse from 309±21 to 168 ± 17 pA ($n = 8$, $p < 0.05$). After washout of the agent, current amplitude returned to 287 ± 19 pA ($n = 8$). In addition to the decreased I_h amplitude, the value of activation time constant (τ_{act}) of the current in response to maintained hyperpolarization was evidently raised as cells were exposed to croton-03 (Figure 1B,C). For example, the presence of 3 μM croton-03 was able to increase the τ_{act} value to 1158 ± 113 msec ($n = 8$, $p < 0.05$) from a control value of 567 ± 54 msec ($n = 8$).
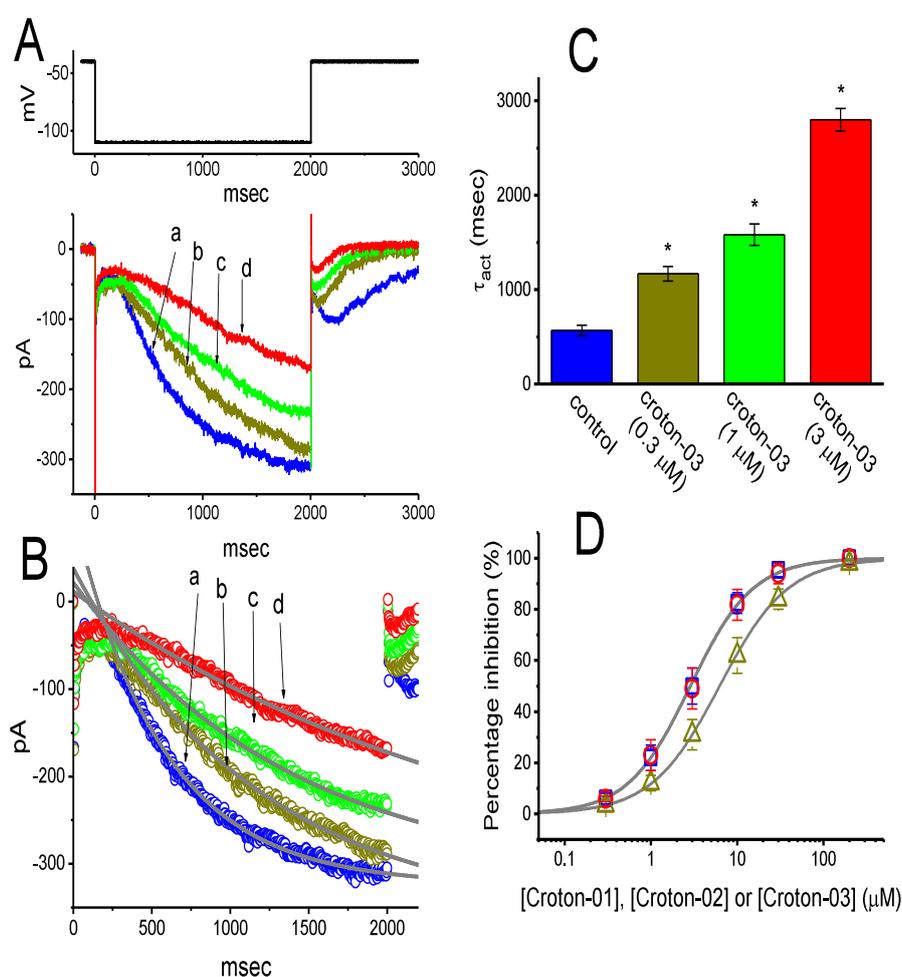
Figure 1. Effects of these *ent*-kaurane-type diterpenoids (i.e., croton-01, croton-02 and croton-03) on hyperpolarization-activated cation current (I_h) recorded from pituitary GH$_3$ cells. Cells were bathed in Ca^{2+}-free Tyrode's solution containing 1 μM tetrodotoxin, the recording pipette was filled with K$^+$-containing solution, and the examined cell was hyperpolarized from −40 to −110 mV (as indicated in the uppermost part of (A)). (**A**) Representative I_h traces obtained in the control (a), and during the exposure to 0.3 μM croton-03 (b), 1 μM croton-03 (c), or 3 μM croton-03 (d). (**B**) Current trajectories fitted by single exponential (indicated in the gray line). a: control; b: 0.3 μM croton-03; c: 1 μM croton-03; d: 3 μM croton-03. For better illustrations, data points in each trace were reduced by a factor of 10. (**C**) Summary bar graph showing the effect of croton-03 on the activation time constant (τ_{act}) of I_h. The I_h was evoked by step hyperpolarization from −40 to −100 mV. (**D**) Concentration-dependent inhibition of I_h by croton-01, croton-02, and croton-03 in GH$_3$ cells. The relations between the percentage inhibition of I_h and the concentrations of croton-01 (O), croton-02 (Δ) or croton-03 (□) are illustrated. Current amplitudes measured at the end of hyperpolarizing step from −40 to −110 mV in the absence or presence of different concentrations of croton-01, croton-02, or croton-03 were compared with the control values. The continuous lines overlaid were fitted by a modified Hill function (see text for details). The IC$_{50}$ values obtained in the presence of croton-01, croton-02, or croton-03 were estimated to be 2.89, 6.25 or 2.84 μM, respectively.

The effects of these diterpenoids (i.e., croton-01, croton-02 and croton-03) on I_h in response to membrane hyperpolarization were further examined and compared in this study. The concentration-dependent relationships among the inhibitory effects of these agents on I_h are illustrated in Figure 1D. The IC$_{50}$ value of croton-01, croton-02, or croton-03 that were required for the inhibition of I_h amplitude was calculated to be 2.89, 6.25, or 2.84 μM, respectively; however, the

Hill coefficients obtained among their effects on I_h did not differ significantly. Therefore, croton-01 or croton-03 tends to be more potent in depressing I_h than croton-02.

2.2. Effects of Croton-03 on I-V Relationship and Steady-State Activation Curve of I_h in GH$_3$ Cells

We further examined the effect of croton-03 on I_h taken at different levels of membrane potentials. The I_h was elicited when the cell was hyperpolarized from −40 to a series of voltage steps ranging between −110 and −30 mV (Figure 2B). Croton-03 at a concentration of 3 μM was able to depress the amplitude of I_h measured at the end of each hyperpolarizing step. The overall *I-V* relationships of I_h with or without addition of croton-03 are shown in Figure 2B. Figure 2C shows the steady-state activation curve of I_h taken with or without addition of croton-03 (3 μM). In control (i.e., in the absence of croton-03), $V_{1/2}$ = −96.2 ± 2.6 mV, q = 3.2 ± 0.8 e (n = 7), while in the presence of 3 μM croton-03, $V_{1/2}$ = −84.3 ± 2.4 mV, q = 3.3 ± 0.7 e (n = 7). Therefore, it is clear from the present results that croton-03 not only led to a conceivable reduction in I_h magnitude, but it also significantly shifted the activation curve along the voltage axis to a more negative potential by approximately 11 mV, irrespectively of minimal change in the gating charge (q) of the curve.
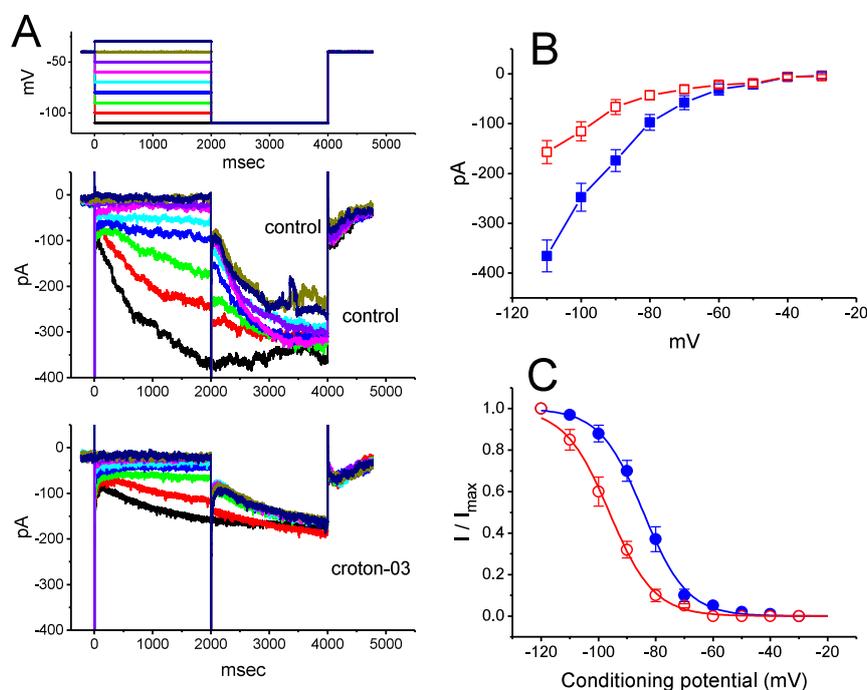
Figure 2. Effect of croton-03 on averaged *I-V* relationship and steady-state activation curve of I_h in GH$_3$ cells. In this set of voltage-clamp current recordings, the conditioning voltage pulses with a duration of 2 sec to potential ranging from −120 and −30 mV. After each conditioning pulse, a test pulse to −110 mV was applied to evoke I_h for measurement of the steady-state activation curve of the current. The upper part of (**A**) indicates the voltage protocol applied. An example of current traces obtained by this two-pulse protocol is illustrated in (**A**). (**B**) Averaged *I-V* relationship of I_h in the control (■) and during the exposure to 3 μM croton-03 (□). Current amplitude was measured at the end of each membrane (i.e., conditioning) potential applied. Each point represents the mean ± SEM (n = 7 for each point). (**C**) Effect of croton-03 on the steady-state activation curve of I_h in the absence (●) and presence (O) of 3 μM croton-03 in GH$_3$ cells. The I_h amplitudes were normalized with those measured at the end of each test pulse and then constructed against the conditioning potentials. The continuous line was least-squares fitted by the Boltzmann equation (see text for details). Please note that the steady-state activation curve of I_h in GH$_3$ cells was significantly shifted toward hyperpolarizing voltage during the exposure to croton-03.

2.3. Effect of Croton-03 on the Voltage-Dependent Hysteresis of I_h Elicited in Response to Long-Lasting Triangular Ramp Pulse

The voltage-dependent hysteresis of ionic currents (e.g., I_h) has been previously demonstrated to exert a significant impact on electrical behaviors such as the firing of action potentials [25–27]. For this reason, we further explored whether there is possible voltage-dependent hysteresis existing in I_h recorded from GH₃ cells. In this series of experiments, we delivered a long-lasting triangular ramp pulse with a duration of 2 sec (i.e., ±0.11 V/sec), as whole-cell mode was firmly established. It is evident from Figure 3A that the trajectories of I_h elicited by the upsloping (i.e., depolarizing from −150 to −40 mV) and downsloping (hyperpolarizing from −40 to −150 mV) ramp pulse as a function of time were distinguishable between them. The current amplitude elicited by the upsloping limb of triangular voltage ramp was significantly greater than that by the downsloping limb, indicating that there is a voltage hysteresis for this current as depicted in Figure 3B, namely the relationship of I_h versus membrane potential. As the ramp speed became reduced, the hysteresis degree for I_h was greatly raised. Of note, as the examined cell was exposed to croton-03 (3 μM), I_h amplitude evoked in the upsloping limb of long-lasting triangular ramp was noted to be decreased to a greater extent than that measured from the downsloping limb. For example, in controls, I_h at the level of -100 mV elicited upon the upsloping and downsloping ends of triangular ramp pulse were 213 ± 23 and 97 ± 12 pA ($n = 7$), respectively, the values of which were found to differ significantly between them ($p < 0.05$). Moreover, in the presence of 3 μM croton-03, the amplitudes of forward and backward I_h taken at the same level of membrane potential were significantly reduced to 136 ± 16 and 58 ± 9 pA ($n = 7$, $p < 0.05$), respectively. However, the magnitude of croton-03-induced current inhibition at the upsloping and downsloping limbs of triangular ramp did not differ significantly, i.e., the presence of 3 μM croton decreased I_h amplitude (at −100 mV) in the upsloping and downsloping limb by about 40%.
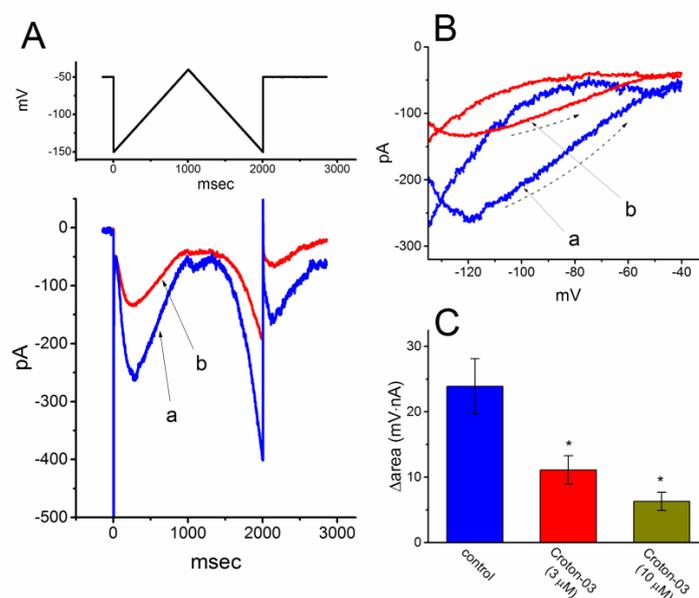
Figure 3. Effect of croton-03 on the voltage hysteresis of I_h recorded from GH₃ cells. (**A**) Representative current trace elicited by long-lasting triangular (i.e., upsloping and downsloping) ramp pulse between −150 and −40 mV with a duration of 2 sec. The upper part in (A) is the voltage protocol applied to the examined cell. Current trace labeled a is control and that labeled b was taken in the presence of 3 μM croton-03. (**B**) Voltage hysteresis (i.e., the relationship of forward and reverse current versus membrane voltage) of I_h measured in the control (a) and during the exposure to 3 μM croton-03 (b). Dashed arrows show the direction of I_h in which time passes during the elicitation of triangular ramp pulse. (**C**) Summary bar graph showing the effect of croton-03 (3 or 10 μM) on the Δarea of voltage hysteresis of I_h (mean ± SEM; $n = 7$ for each bar). * Significantly different from control ($p < 0.05$).

We next quantified the degree of voltage-dependent hysteresis based on the difference in area under the curve in the forward (upsloping) and reverse (downsloping) direction as described by the arrows in Figure 3B. It was seen that for I_h identified in GH$_3$ cells, the degree of voltage hysteresis increased with slower ramp speed, and that the presence of croton-03 led to a considerable reduction in the amount of such hysteresis. For example, as the duration of triangular ramp was prolonged from 2 to 3 sec, the area under the curve between forward and backward current traces (i.e., Δarea) increased from 23.9 ± 4.2 to 34.1 ± 4.9 mV·pA, ($n = 7$, $p < 0.05$). Figure 3C illustrates summary of the data showing effects of croton-03 at the different concentrations on the area under such curve. For example, apart from its depression of I_h magnitude, addition of croton-03 (3 μM) significantly decreased the area by about 50% elicited in response to such long-lasting triangular voltage ramp, as demonstrated by a significant decrease of Δarea from 23.9 ± 4.2 to 11.1 ± 2.2 mV·nA ($n = 7$, $p < 0.05$).

2.4. Effect of Croton-03, YS-035, Zatebradine, Croton-03 Plus SQ-22536, and Croton-03 Plus Oxaliplatin on I_h Amplitude

The extracts from *C. zehntneri* such as anethole and estragole were demonstrated to produce an increase in the level of intracellular cyclic AMP in the copora cavernosa smooth muscle [28]. In the next set of experiments, we examined and compared the effects of croton-03, YS-035, zatebradine, croton-03 plus SQ-22536, and croton-03 plus oxaliplatin on I_h amplitude in GH$_3$ cells. YS-035 or zatebradine was recognized as an inhibitor of I_h [19,29], oxaliplatin was recently demonstrated to stimulate I_h [30,31], and SQ-22536 is an inhibitor adenylate cyclase. As illustrated in Figure 4, similar to the effect of croton-03 on I_h described above, the addition of either YS-053 (3 μM) or zatebradine (3 μM) was effective at depressing I_h amplitude. Subsequent application of SQ-22536 (10 μM), still in the presence of croton-03, had minimal effect on I_h produced by croton-03; however, further addition of oxaliplatin (10 μM) significantly attenuated croton-03-mediated inhibition of I_h. Alternatively, chlorotoxin (1 μM), an inhibitor of Cl$^-$ channels, did not depress I_h amplitude effectively (data not shown). Consequently, the experimental results led us to indicate that croton-03-mediated depression of I_h appears to be independent of its increase in intracellular cyclic AMP, though it is sensitive to be reversed by further addition of oxaliplatin.
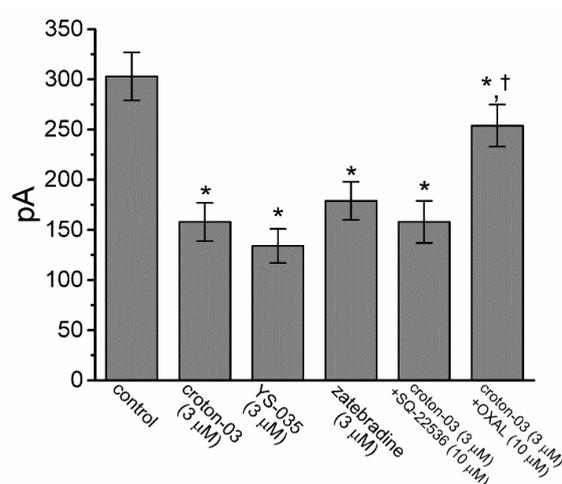
Figure 4. Comparisons among effects of croton-03, YS-035, zatebradine, croton-03 plus SQ-22536 and croton-03 plus oxaliplatin (OXAL) on I_h amplitude recorded from GH$_3$ cells. Cells were bathed in Ca^{2+}-free Tyrode's solution and the hyperpolarizing potential from −40 to −110 mV with a duration of 2 sec was applied to the cell. I_h amplitude was measured at the end of hyperpolarizing pulse in the presence of different tested compounds. Each bar indicates the mean±SEM ($n = 7$–9). * Significantly different from control ($p < 0.05$) and † significantly different from croton-03 (3 μM) along group ($p < 0.05$).

2.5. Effect of Croton-03 on erg-Mediated K⁺ Current (I_{K(erg)}) in GH₃ Cells

In another set of current recordings, we investigated the possible modification of croton-03 on $I_{K(erg)}$. In these experiments, we bathed cells in high-K^+, Ca^{2+}-free solution and, during the measurements, we filled the pipette solution by using K^+-containing solution. As the whole-cell current recordings were achieved, the examined cell was maintained at the level of -10 mV and a long-step membrane hyperpolarization was applied. As illustrated in Figure 5, the addition of croton-03 at a concentration of 3 or 10 μM slightly depressed the amplitude of deactivating $I_{k(erg)}$, the biophysical or pharmacological properties of which were previously described [32]. However, minimal change in the decaying time course of $I_{K(erg)}$ in response to membrane hyperpolarization was demonstrated in the presence of croton-03. The concentration-dependent inhibition of croton-03 on $I_{K(erg)}$ was then constructed with an IC$_{50}$ value of 35.3 μM, which is higher than that for the inhibition of I_h described above. As such, the $I_{k(erg)}$ identified in GH₃ is relatively resistant to depression by the presence of croton-03.
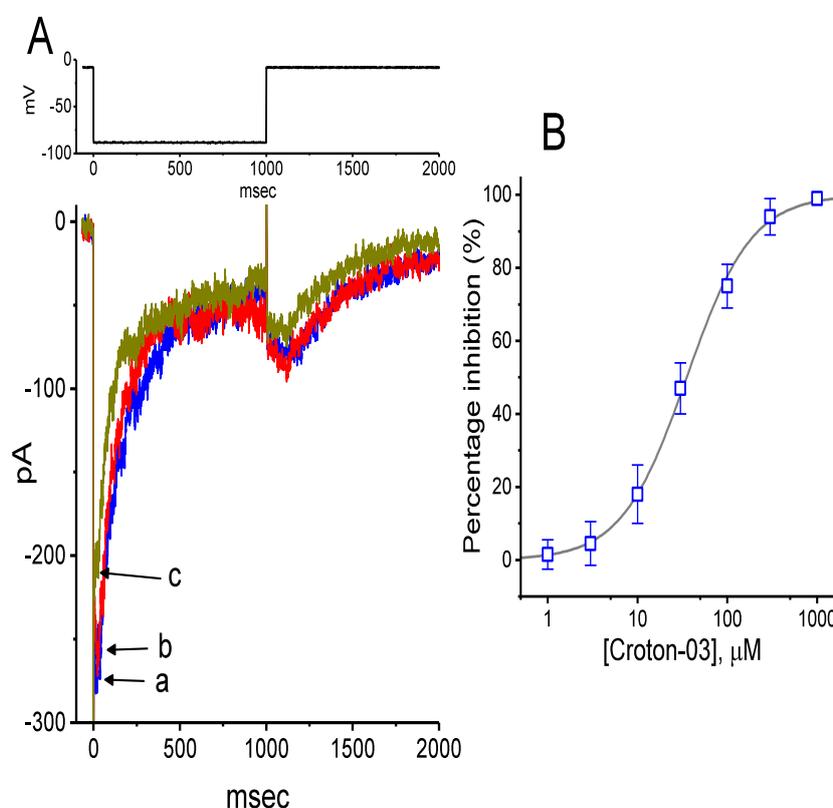
Figure 5. Effect of croton-03 on *erg*-mediated K⁺ current ($I_{K(erg)}$) in GH₃ cells. In these experiments, cells were bathed in Ca^{2+}-free, high-K^+ solution, and the electrode was filled with K^+-containing solution. (**A**) Representative $I_{K(erg)}$ traces obtained in the control (a) and during the exposure to 3 μM croton-03 (b) or 10 μM croton-03 (c). The upper part indicates the voltage protocol applied. (**B**) Concentration-dependent inhibition by croton-03 of $I_{K(erg)}$ amplitude (mean ± SEM; *n* = 7–8 for each point). Each cell was hyperpolarized from −10 to −90 mV and current amplitudes obtained during the exposure to different croton-03 concentrations were measured at the beginning of each hyperpolarizing step. The smooth curve was least-squares fitted by the Hill equation (see text for details), and the IC$_{50}$ value was constructed and then estimated to be 35.3 μM.

2.6. Effect of Croton-03 on Sag Potential Measured from GH₃ Cells

We further performed current-clamp voltage recordings in attempts to test if croton-03 could produce any perturbations on sag potential in these cells. Sag potential in response to hyperpolarizing

current stimulus has been described to be intimately linked to the occurrence of I_h in different types of central neurons [20,33,34]. As shown in Figure 6, under our experimental condition, when the whole-cell voltage recordings were firmly established, a long-step hyperpolarizing current injection with the amplitude of around 25 pA was found to induce sag potential (i.e., drop down to a lower level in the membrane potential upon hyperpolarizing current stimuli). The addition of ivabradine (3 μM), an inhibitor of I_h, was effective at depressing the amplitude of sag potential. Moreover, the presence of 1 or 3 μM croton-03 produced an effective depression of sag potential elicited by hyperpolarizing current stimulus. For example, croton-03 at a concentration of 3 μM decreased the amplitude of sag potential from 29.2 ± 2.1 to 18.3 ± 1.5 mV ($n = 8$, $p < 0.05$). Therefore, the sag potential identified in GH$_3$ cells is connected with the magnitude of I_h and the depression of such potential caused by the presence of croton-03 could result largely from its inhibitory effect on I_h observed in GH$_3$ cells.
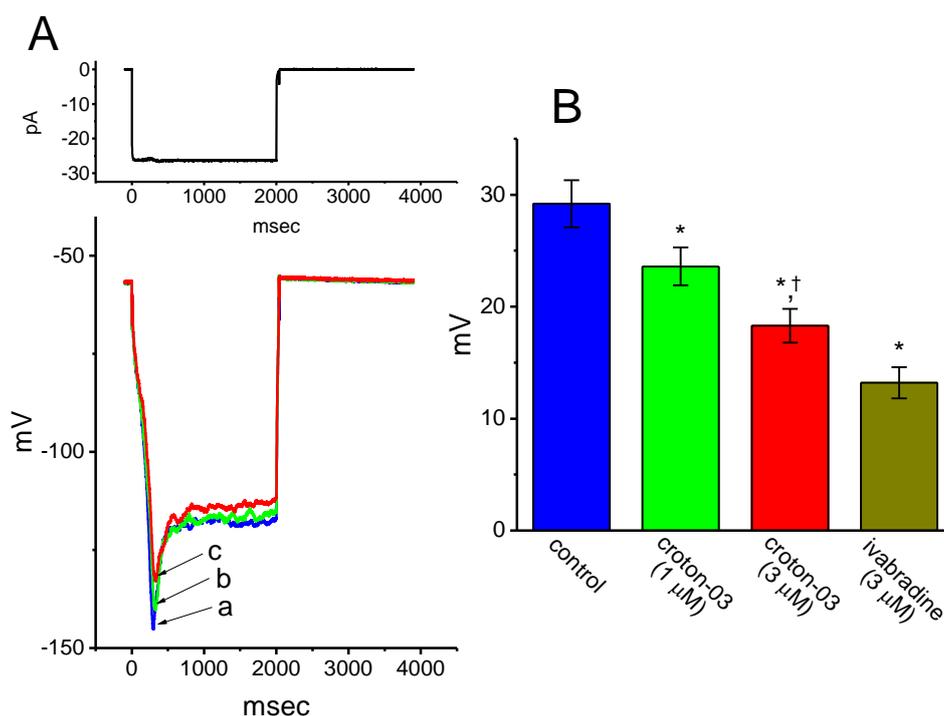
Figure 6. Effect of croton-03 on sag potential identified in GH$_3$ cells. Cells were bathed normal Tyrode' solution containing 1.8 mM CaCl$_2$ and 1 μM tetrodotoxin. Current-clamp voltage recordings were made in these experiments and a long-step hyperpolarizing (i.e., inward) current stimulus was applied to the examined cell. (**A**) Superimposed potential traces obtained in the control (a) and during cell exposure to 1 μM croton-03 (b) or 3 μM croton-03 (c). Upper part indicates the long-step current injection applied. (**B**) Summary bar graph showing the effect of croton-03 or ivabradine on the amplitude of sag potential (mean $\pm$ SEM; $n = 6$–8 for each bar). The amplitude of sag potential (i.e., difference between the beginning and end of hyperpolarizing stimulus) was taken in the absence and presence of croton-03 or ivabradine. * Significantly different from control ($p < 0.05$) and † significantly different from croton-03 (1 μM) along group ($p < 0.05$).

2.7. Inhibitory Effect of Croton-03 on I_h in INS1 Insulin-Secreting Cells

The biophysical or pharmacological properties of I_h observed in GH$_3$ cells may be distinguishable from those in other types of endocrine cells. Previous studies have demonstrated the presence of I_h or delayed-rectifier K$^+$ current in pancreatic β-cells [35,36]. INS-1 cells have retained some characteristics of normal pancreatic β-cells [37]. In another set of whole-cell current recordings, we thus further attempted to test whether croton-03 is capable of perturbing ionic currents (e.g., I_h or $I_{K(erg)}$) present in INS-1 insulin-secreting cells. As illustrated in Figure 7, indistinguishable from the observations

made in GH_3 cells, the presence of croton-03 effectively depressed the amplitude of I_h in response to long-step membrane hyperpolarization. Moreover, subsequent addition of oxaliplatin (10 µM), still in the presence of croton-03 (3 µM), could significantly attenuate croton-03-mediated inhibition of the I_h amplitude. Oxaliplatin was previously demonstrated to stimulate I_h amplitude [30,31].
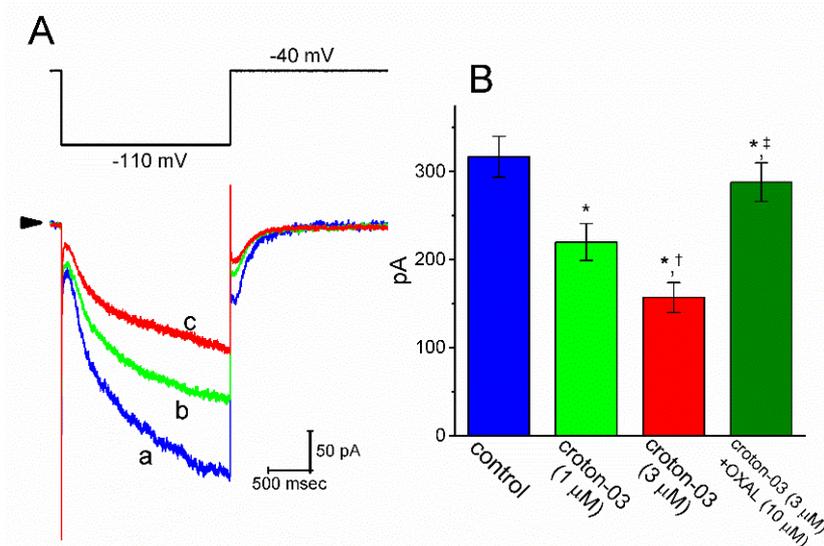
Figure 7. Inhibitory action of croton-03 on I_h identified in INS-1 cells. This set of experiments was conducted in cells bathed in Ca^{2+}-free, Tyrode's solution and the recording pipette was filled with K^+-containing solution. (**A**) Representative I_h traces obtained in the absence (a) and presence of 1 µM croton-03 (b) or 3 µM croton-03 (c). The upper part indicates the voltage protocol applied. (**B**) Summary bar graph showing the effect of croton-03 and croton-03 plus oxaliplatin on I_h amplitude (mean ± SEM; n = 7–8 for each bar). Current amplitude was obtained at the end of 2-sec hyperpolarizing pulse from −10 to −110 mV. OXAL: 10 µM oxaliplatin. * Significantly different from control ($p < 0.05$), † significantly different from croton-03 (1 µM) along group ($p < 0.05$), and ‡ significantly different from croton-03 (3 µM) along group ($p < 0.05$).

2.8. Effect of Croton-03 on $I_{K(erg)}$ Identified in INS1 Cells

The $I_{K(erg)}$ identified in INS-1 cells was also tested to evaluate whether croton-03 has any effect on this current. Cells were bathed in high-K^+, Ca^{2+}-free solution, and the recording pipette was filled with K^+-containing solution. As illustrated in Figure 8, when the membrane potential was hyperpolarized from −10 to −140 mV, the deactivating $I_{K(erg)}$ was readily evoked in these cells. Moreover, within 2 min of exposing to croton-03 at a concentration of 10 or 30 µM, the $I_{k(erg)}$ amplitude elicited by step hyperpolarization was robustly reduced. For example, the addition of croton-03 (30 µM) decreased current amplitude measured at the beginning of hyperpolarizing pulse from 984 ± 43 to 713 ± 28 pA (n = 8, $p < 0.05$). Hence, in keeping with the observations described above in GH_3 cells, the $I_{K(erg)}$ identified in INS-1 cells was subject to be mildly but significantly depressed by croton-03.
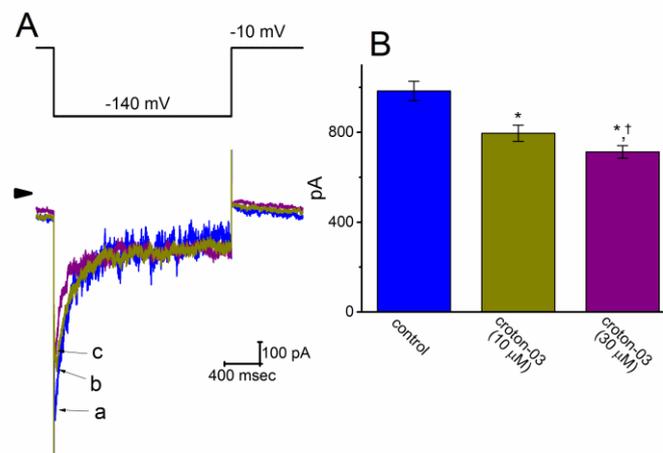
Figure 8. Effect of croton-03 on $I_{K(erg)}$ amplitude in INS-1 cells. In these experiments, we bathed in Ca^{2+}-free, high-K^+ solution and, during the measurements, we filled the pipette by using K^+-containing solution. (**A**) Representative $I_{K(erg)}$ traces elicited in response to 1-sec step hyperpolarization from −10 to −140 mV (as indicated in the upper part). The current trace labeled a is control, and those labeled b or c were obtained in the presence of 10 or 30 μM croton-03, respectively. Arrowhead indicates the zero current level and calibration mark shown in the right lower side applies all current traces. (**B**) Summary bar graph of croton-03 effects on the amplitude of deactivating $I_{K(erg)}$ elicited by membrane hyperpolarization (mean ± SEM; $n = 8$ for each bar). Current amplitude was taken at the beginning of each hyperpolarizing pulse. * Significantly different from control ($p < 0.05$) and [†] significantly different from croton-03 (10 μM) alone group ($p < 0.05$).

3. Discussion

The principal findings in this study were as follows: (1) the presence of croton-01, croton-02, or croton-03 produced concentration-dependent inhibition of I_h in pituitary GH_3 cells with effective IC_{50} of 2.89, 6.25 or 2.84 μM, respectively.; (2) croton-03 shifted the steady-state activation curve of I_h toward a more negative potential; (3) croton-03 decreased the voltage-dependent hysteresis of I_h and further addition of SQ-22536 did not alter croton-03-mediated inhibition of I_h; (4) croton-03 mildly depressed the amplitude of $I_{K(erg)}$; (5) croton-03 decreased the amplitude of sag potential elicited by hyperpolarizing current stimulus; and (6) croton-03 also depressed I_h amplitude in INS-1 insulin-secreting cells.

A previous report has demonstrated the ability of extracts from *C. zehntneri* (i.e., anethole and estragole) to increase the levels of cyclic AMP in corpora cavernosa smooth muscle [28]. However, in continued presence of croton-03, further addition of SQ-22536, an inhibitor of adenylate cyclase, was unable to attenuate croton-03-mediated depression of I_h seen in GH_3 cells. Therefore, croton-03-induced block of I_h is unlikely to ascribe largely from changes in the level of intracellular cyclic AMP.

In light of the steady-state activation curve of I_h during the exposure of croton-03, the voltage for half-maximal activation was noted to be in the range of the firing of action potentials. The activation time course of I_h observed at the different level of voltages became slower in the presence of croton-03. Therefore, it is conceivable that the croton-03 molecule has a higher affinity toward the open state of HCN channels than toward the closed or resting state of the channels identified in GH_3 or INS-1 cells. As such, the magnitude of croton-03-induced block on I_h tends to be voltage-dependent, and any changes in I_h amplitude caused by croton-03 would fairly rely on the croton-03 concentration applied, the firing of action potentials, and the pre-existing level of membrane potential.

The voltage-dependent hysteresis of I_h has been shown to exhibit substantial role in influencing electrical behavior of electrically excitable cells such as GH_3 cells. In keeping with previous observations [25–27], the I_h identified in GH_3 cells was found to undergo either a hysteresis in its voltage dependence, or mode shift in which the voltage sensitivity of gating charge movements

relies on the previous state [26,27]. In this study, we also examined possible perturbations of croton-03 on such non-equilibrium property of I_h in GH$_3$ cells. Our results clearly demonstrated that the presence of this diterpenoid (croton-03) was capable of diminishing such hysteresis involved in the voltage-dependent elicitation of I_h.

In this study, the effective IC$_{50}$ of croton-03 required for the inhibition of I_h seen in GH$_3$ cells was 2.84 μM, a value that is similar to that of croton-01, but slightly lower than that of croton-02. This discrepancy remains unclear; however, it could be related to the possibility that croton-03 is assumed to be more hydrophobic than croton-01 or croton-02. The presence of croton-03 was also noted to depress the activation time course of I_h as well as to shift the activation curve of the current to a more depolarized potential. Regardless of the detailed mechanism of its inhibitory actions, the I_h (or HCN-encoded current) could conceivably be an important target of these diterpenoids such as croton-3, which can interact with the HCN channel to decrease the amplitude of I_h in endocrine cells such as GH$_3$ and INS-1 cells. The present results also imply the possibility of its perturbations on different cell types which express functional HCN channels such as sensory neurons [38,39]. Indeed, our results demonstrated that subsequent addition of oxaliplatin, but still in the presence of croton-03, could significantly attenuate croton-03-mediated inhibition of I_h in GH$_3$ and INS-1 cells. Oxaliplatin, an activator of I_h, was recognized as a chemotherapy-induced neuropathic pain [30,31].

It needs to be mentioned that the IC$_{50}$ value (i.e., 2.84 μM) estimated for croton-03-mediated inhibition of I_h tends to be so high that it may be reached anywhere in the organism upon consumption of even large amounts of *C. tonkinensis*. Therefore, to what extent the results observed herein have a real physiological, nutrition-related relevance remains to be further investigated.

The I_h has been recognized to be carried by channels of the HCN gene family, namely HCN1, HCN2, HCN3 and HCN4 [10]. It has been recently demonstrated that HCN1, HCN2 or HCN3 channels play essential roles in sensory excitability and pain sensation [30,38,40]. Regardless of the detailed mechanism of their inhibitory actions, there is likely to be a relevant link between the effects of these croton derivatives on electrically excitable cells and their inhibitory effects on HCN channel activity, though croton-03-mediated effect on HCN channels might not be isoform-specific. It is tempting to speculate that the blocking by these *ent*-kaurane-type diterpenoids of I_h plays an important role in modulating the functional activities of neurons and neuroendocrine or endocrine cells [5,6]. Therefore, croton derivatives and other structurally related *ent*-kaurane-type diterpenoids would be the harbinger of intriguing compounds that use the open/activated state of the HCN channels as a substrate. Our study strongly suggests that these *ent*-kaurane diterpenoids should somehow act on cellular mechanisms through which they exert high influence on the functional activities of endocrine or neuroendocrine cells.

4. Materials and Methods

4.1. Purification, Extraction, and Fractionation of Plant Materials

The general procedures follow those shown in the previous research [41]. The whole *C. tonkinensis* Gagnep (Euphorbiaceae) plant has been collected in Vietnam, and the plant material was identified and authenticated by Vu Xuan Phuong, Institute of Ecology and Biological Resources, Vietnamese Academy of Science and Technology, Hanoi, Vietnam. A voucher specimen (Viet-TSWu-2009-0901-001) was deposited in the herbarium of the Institute of Ecology and Biological Resources, Vietnamese Academy of Science and Technology.

Extraction and fractionation were performed as described previously [41]. Briefly, air-dried and powdered whole plants of *C. tonkinensis* were extracted with methanol and concentrated to form brown syrup. The *n*-hexane soluble fraction was subjected to silica gel column chromatography eluted with a step gradient to afford 19 fractions (H1-H19). Minor fractions in subfraction H13-4, H15-2-2 and H15-3-3 were recrystallized with chloroform methanol to yield croton-01, croton-03, and croton-02, respectively.

4.2. Drugs, Chemicals, and Solutions

The chemical structures of croton-01 (*ent*-18-acetoxy-7α-hydroxykaur-16-en-15-one), croton-02 (*ent*-7α,14β-dihydroxykaur-16-en-15-one) and croton-03 (*ent*-1β-acetoxy-7α,14β-dihydroxykaur-16-en-15-one) were described previously [41,42]. β-Mercaptoethanol and tetrodotoxin were acquired from Sigma-Aldrich (St. Louis, MO), ivabradine, SQ-22536, YS-035 and zatebradine were from Tocris (Bristol, UK), and oxaliplatin was from Sanofi-Aventis (New York, NY, USA). Chlorotoxin was kindly provided by Professor Dr Woei-Jer Chuang (Department of Biochemistry, National Cheng Kung University Medical College, Tainan, Taiwan). Cell culture media such as Ham's F-12 or RPMI-1640 medium, fetal bovine or calf serum, and horse serum were acquired from Invitrogen (Carlsbad, CA, USA), unless stated otherwise, while other chemicals or solvents such as methanol, HEPES, and aspartic acid, were of analytical reagent grade. The twice-distilled water that had been de-ionized through a Millipore-Q system (APS Water Services Inc., Van Nuys, CA, USA) was used in all experiments.

The composition of bath solution (i.e., HEPES-buffered normal Tyrode's solution) was as follows (in mM): NaCl 136.5, KCl 5.4, $CaCl_2$ 1.8, $MgCl_2$ 0.53, glucose 5.5, and HEPES-NaOH buffer 5.5 (pH 7.4). To measure membrane potential or K^+ currents (i.e., $I_{K(erg)}$) or I_h, we filled the patch pipette with a solution (in mM): KCl 140, $MgCl_2$ 1, Na_2ATP 3, Na_2GTP 0.1, EGTA 0.1, and HEPES-KOH buffer 5 (pH 7.2). To record $I_{K(erg)}$, we bathed GH$_3$ or INS-1 cells in high-K^+, Ca^{2+}-free solution (in mM): KCl 145, $MgCl_2$ 0.53, and HEPES-KOH 5 (pH 7.4). The pipette solution and culture media were commonly filtered on the day of use with sterile Acrodisc® filter with 0.2-μm Supor® membrane (Pall Corp., Port Washington, NY, USA).

4.3. Cell Preparations

GH$_3$ pituitary tumor cells, obtained from the Bioresources Collection and Research Center ([BCRC-60015]; Hinchu, Taiwan), were routinely maintained in Ham's F-12 media supplemented with 15% horse serum (*v/v*), 2.5% fetal calf serum (*v/v*), and 2 mM L-glutamine [14]. The rat INS-1 cell line (clone 832/13) was kindly provided by Christopher B. Newgard, Duke University, Durham, NC. Cells were plated in 10-cm plate and grown in RPMI-1640 medium supplemented with 11.1 mM D-glucose, 10% fetal bovine serum, 10 mM HEPES, 2 mM L-glutamine, 1 mM sodium pyruvate, and 50 μM β-mercaptoethanol [34]. The experiments were commonly made five or six days after cells had been cultured (60–80% confluence).

4.4. Electrophysiological Measurements

Shortly before each experiment, cells (i.e., GH$_3$ or INS-1 cells) were dissociated and a few drops of cell suspension was transferred to a home-made chamber mounted on the fixed stage of an inverted Diaphot-200 microscope (Nikon, Tokyo, Japan). They were immersed at room temperature (20–25 °C) in normal Tyrode's solution, the composition of which is described above. We fabricated the recording electrode from Kimax-51 glass capillaries (#34500; Kimble, Vineland, NJ) using a PP-830 vertical puller (Narishige, Tokyo, Japan) in which a two-step pull mechanism was applied, and their tips were fire-polished with a microforge (MF-83, Narishige). During the measurements, the electrode with tip resistance ranging from 3 to 5 MΩ, which was firmly inserted into holder, was maneuvered by use of a WR-98 micromanipulator (Narishige). Patch-clamp experiments operated under voltage- or clamp-clamp mode were carried out by using an RK-400 patch-clamp amplifier (Bio-Logic, Claix, France) connected with a personal computer [43]. Shortly before giga-seal formation was achieved, the potentials were commonly corrected for the liquid junction potential that generally developed at the pipette tip, as the composition of internal solution was different from that in the bath.

4.5. Data Recordings

The data comprising both potential and current traces were collected online and stored in an HP Pavilion ×360 touchscreen laptop computer (14-cd1053TX; Hewlett-Packard, Palo Alto, CA, USA) at 10 kHz equipped with the 12-bit Digidata 1440A interface (Molecular Devices, Sunnyvale, CA, USA). The latter device was widely accepted and used for efficient analog-to-digital/digital-to-analog conversion. During the experiments, the data acquisition system was driven by pCLAMP 10.7 software (Molecular Devices) run under Windows 10 (Redmond, WA, USA), and the current/voltage signals were also simultaneously monitored on LCD monitor (MB169B+; ASUS, Taipei, Taiwan) through a USB type-C connection. Current signals were low-pass filtered at 2 kHz with an FL-4 four-pole Bessel filter (Dagan, Minneapolis, MN, USA). Through digital-to-analog conversion, the pCLAMP-generated voltage-clamp patterns with different rectangular, triangular or linear ramp waveforms were designed beforehand, in attempts to determine the current-voltage (*I-V*) relationships for different types of ionic currents such as I_h, and the steady-state activation curve of I_h.

4.6. Data Analyses

To determine percentage inhibition of croton-01, croton-02, or croton-03 on I_h, each cell was hyperpolarized from −40 to −120 with a duration of 2 s, while to evaluate that of croton-03 on $I_{K(erg)}$, the cell was hyperpolarized from −10 to −90 mV. The I_h or $I_{K(erg)}$ amplitudes respectively measured at the end or beginning of each hyperpolarizing step in the presence of different concentrations of compounds were compared with the control value (i.e., in the absence of any agent). The concentration-dependent effects of these compounds on the inhibition of I_h or $I_{K(erg)}$ amplitude seen in GH$_3$ cells were fitted with the goodness of fit to a modified Hill function by 64-bit OriginPro 2016 (OriginLab); that is,

$$\text{Percentage inhibition } (\%) = \frac{E_{max} \times [C]^{n_H}}{[C]^{n_H} + IC_{50}^{n_H}} \tag{1}$$

where [C] is the concentration of croton-01, croton-2, or croton-03; IC_{50} and n_H are the concentration required for a 50% inhibition and the Hill coefficient, respectively; and E_{max} is the maximal inhibitions of I_h or $I_{k(erg)}$ amplitude produced by each tested compound.

To evaluate the effect of croton-03 on the steady-state activation of I_h, the relationships between the normalized amplitude of I_h and the conditioning potentials obtained in the absence and presence of 3 μM croton-03 were least-squares fitted with a Boltzmann function of the following form:

$$I = \frac{I_{max}}{1 + exp\left[\frac{-(V-V_\frac{1}{2})qF}{RT}\right]} \tag{2}$$

where I_{max} is the maximal amplitude of I_h taken with or without addition of 3 μM croton-03 at the conditioning potential of −30 mV, $V_{1/2}$ the voltage at which half-maximal activation occurs, q the apparent gating charge, F Faraday's constant, R the universal gas constant, and T the absolute temperature.

4.7. Statistical Analyses

Linear or nonlinear curve fitting to data shown here was performed by using either OriginPro 2016 (OriginLab, Northampton, MA) or the Solver subroutine embedded in Excel 2016 (Microsoft) [44]. The data are presented as mean±standard errors of the mean (SEM) and error bars were plotted as SEM. Values of *n* indicate the number of cells obtained. The paired or unpaired Student's *t*-test and one-way analysis of variance (ANOVA) followed by the least significance difference method for multiple comparisons were used for the statistical evaluation of differences among means. Non-parametric Kruskal-Wallis test would be implemented, as the assumption of normality underlying ANOVA was

violated. Statistical analyses were generally made using Statistical Package for the Social Sciences version 20 (SPSS, IBM Corp., Armonk, NY, USA). The level of statistical significance was set at $p < 0.05$.

Author Contributions: Conceptualization, P.-C.K. and S.-N.W.; methodology, P.-C.K., Y.-C.L. (Yen-Chin Liu) and Y.-C.L. (Yi-Ching Lo); software, S.-N.W.; validation, P.-C.K. and S.-N.W.; formal analysis, Y.-C.L. (Yen-Chin Liu) and S.-N.W.; investigation, S.-N.W.; resources, P.-C.K. and S.-N.W.; data curation, P.-C.K. and S.-N.W.; writing—original draft preparation, P.-C.K. and Y.-C.L. (Yen-Chin Liu); writing—review and editing, S.-N.W. and Y.-C.L.(Yi-Ching Lo); visualization, S.-N.W.; supervision, S.-N.W.; project administration, P.-C.K. and S.-N.W.; funding acquisition, P.-C.K. and S.-N.W.. All authors have read and agreed to the published version of the manuscript

Abbreviations

croton-01	*ent*-18-acetoxy-7α-hydroxykaur-16-en-15-one
croton-02	*ent*-7α,14β-dihydroxykaur-16-en-15-one
croton-03	*ent*-1β-acetoxy-7α,14β-dihydroxykaur-16-en-15-one
erg	*ether-à-go-go*-related gene
HCN channel	hyperpolarization-activated, cyclic nucleotide-gated channel
I-V	current versus voltage
IC$_{50}$	the concentration required for 50% inhibition
I_h	hyperpolarization-activated cation current
$I_{K(erg)}$	*erg*-mediated K$^+$ current
act	activation time constant

References

1. Giang, P.M.; Son, P.T.; Lee, J.J.; Otsuka, H. Four ent-kaurane-type diterpenoids from Croton tonkinensis Gagnep. *Chem. Pharm. Bull.* **2004**, *52*, 879–882. [CrossRef] [PubMed]

2. Neves, J.R.; Lira, G.H.; Oliveira Neto, R.M.; Graca, J.R.; Vasconcelos, P.R.; Nobre e Souza, M.A.; Magalhaes, P.J.; Rola, F.H.; Santos, A.A. 1.8 cineole decreases gastric compliance in anesthetized rats. *Acta Cir. Bras.* **2007**, *22*, 63–67. [CrossRef] [PubMed]

3. de Siqueira, R.J.; Magalhaes, P.J.; Leal-Cardoso, J.H.; Duarte, G.P.; Lahlou, S. Cardiovascular effects of the essential oil of Croton zehntneri leaves and its main constituents, anethole and estragole, in normotensive conscious rats. *Life Sci.* **2006**, *78*, 2365–2372. [CrossRef]

4. de Siqueira, R.J.; Duarte, G.P.; Magalhaes, P.J.; Lahlou, S. Cardiovascular effects of the essential oil of Croton zehntneri leaves in DOCA-salt hypertensive, conscious rats. *Nat. Prod. Commun.* **2013**, *8*, 1167–1170. [CrossRef] [PubMed]

5. Leal-Cardoso, J.H.; Lahlou, S.; Weinreich, D.; Caldas Magalhaes, P.J. The essential oil of Croton nepetaefolius selectively blocks histamine-augmented neuronal excitability in guinea-pig celiac ganglion. *J. Pharm. Pharmacol.* **2010**, *62*, 1045–1053. [CrossRef]

6. Aguiar, L.A.; Porto, R.S.; Lahlou, S.; Ceccatto, V.M.; Barbosa, R.; Lemos, T.L.; dos Santos, H.S.; Coelho-de-Souza, A.N.; Magalhaes, P.J.; Zin, W.A.; et al. Antispasmodic effects of a new kaurene diterpene isolated from Croton argyrophylloides on rat airway smooth muscle. *J. Pharm. Pharmacol.* **2012**, *64*, 1155–1164. [CrossRef]

7. Fischer, H.; Machen, T.E.; Widdicombe, J.H.; Carlson, T.J.; King, S.R.; Chow, J.W.; Illek, B. A novel extract SB-300 from the stem bark latex of Croton lechleri inhibits CFTR-mediated chloride secretion in human colonic epithelial cells. *J. Ethnopharmacol.* **2004**, *93*, 351–357. [CrossRef]

8. Tradtrantip, L.; Namkung, W.; Verkman, A.S. Crofelemer, an antisecretory antidiarrheal proanthocyanidin oligomer extracted from Croton lechleri, targets two distinct intestinal chloride channels. *Mol. Pharmacol.* **2010**, *77*, 69–78. [CrossRef]

9. Belardinelli, L.; Giles, W.R.; West, A. Ionic mechanisms of adenosine actions in pacemaker cells from rabbit heart. *J. Physiol.* **1988**, *405*, 615–633. [CrossRef]

10. DiFrancesco, D. Serious workings of the funny current. *Prog. Biophys. Mol. Biol.* **2006**, *90*, 13–25. [CrossRef]

11. Hao, X.M.; Xu, R.; Chen, A.Q.; Sun, F.J.; Wang, Y.; Liu, H.X.; Chen, H.; Xue, Y.; Chen, L. Endogenous HCN channels modulate the firing activity of globus pallidus neurons in Parkinsonian animals. *Front. Aging Neurosci.* **2019**, *11*, 190. [CrossRef] [PubMed]

12. He, C.; Chen, F.; Li, B.; Hu, Z. Neurophysiology of HCN channels: From cellular functions to multiple regulations. *Prog. Neurobiol.* **2014**, *112*, 1–23. [CrossRef] [PubMed]

13. Irisawa, H.; Brown, H.F.; Giles, W. Cardiac pacemaking in the sinoatrial node. *Physiol. Rev.* **1993**, *73*, 197–227. [CrossRef] [PubMed]

14. Liu, Y.C.; Wang, Y.J.; Wu, P.Y.; Wu, S.N. Tramadol-induced block of hyperpolarization-activated cation current in rat pituitary lactotrophs. *Naunyn. Schmiedebergs Arch. Pharmacol.* **2009**, *379*, 127–135. [CrossRef]

15. McKinley, J.W.; Shi, Z.; Kawikova, I.; Hur, M.; Bamford, I.J.; Sudarsana Devi, S.P.; Vahedipour, A.; Darvas, M.; Bamford, N.S. Dopamine deficiency reduces striatal cholinergic interneuron function in models of Parkinson's disease. *Neuron* **2019**, *103*, 1056–1072.e6. [CrossRef]

16. Spinelli, V.; Sartiani, L.; Mugelli, A.; Romanelli, M.N.; Cerbai, E. Hyperpolarization-activated cyclic-nucleotide-gated channels: Pathophysiological, developmental, and pharmacological insights into their function in cellular excitability. *Can. J. Physiol. Pharmacol.* **2018**, *96*, 977–984. [CrossRef]

17. Stojilkovic, S.S.; Tabak, J.; Bertram, R. Ion channels and signaling in the pituitary gland. *Endocr. Rev.* **2010**, *31*, 845–915. [CrossRef]

18. Hsiao, H.T.; Liu, Y.C.; Liu, P.Y.; Wu, S.N. Concerted suppression of I_h and activation of $I_{K(M)}$ by ivabradine, an HCN-channel inhibitor, in pituitary cells and hippocampal neurons. *Brain Res. Bull.* **2019**, *149*, 11–20. [CrossRef]

19. Romanelli, M.N.; Cerbai, E.; Dei, S.; Guandalini, L.; Martelli, C.; Martini, E.; Scapecchi, S.; Teodori, E.; Mugelli, A. Design, synthesis and preliminary biological evaluation of zatebradine analogues as potential blockers of the hyperpolarization-activated current. *Bioorg. Med. Chem.* **2005**, *13*, 1211–1220. [CrossRef]

20. Mellon, D., Jr. Electrophysiological evidence for intrinsic pacemaker currents in crayfish parasol cells. *PLoS ONE* **2016**, *11*, e0146091. [CrossRef]

21. Tigerholm, J.; Poulsen, A.H.; Andersen, O.K.; Morch, C.D. From perception threshold to ion channels-a computational study. *Biophys. J.* **2019**, *117*, 281–295. [CrossRef] [PubMed]

22. Carvalho, J.C.; Silva, M.F.; Maciel, M.A.; Pinto, A.C.; Nunes, D.S.; Lima, R.M.; Bastos, J.K.; Sarti, S.J. Investigation of anti-inflammatory and antinociceptive activities of trans-dehydrocrotonin, a 19-nor-clerodane diterpene from Croton cajucara. Part 1. *Planta Med.* **1996**, *62*, 402–404. [CrossRef] [PubMed]

23. Cordeiro, K.W.; Felipe, J.L.; Malange, K.F.; do Prado, P.R.; de Oliveira Figueiredo, P.; Garcez, F.R.; de Cassia Freitas, K.; Garcez, W.S.; Toffoli-Kadri, M.C. Anti-inflammatory and antinociceptive activities of Croton urucurana Baillon bark. *J. Ethnopharmacol.* **2016**, *183*, 128–135. [CrossRef] [PubMed]

24. Simasko, S.M.; Sankaranarayanan, S. Characterization of a hyperpolarization-activated cation current in rat pituitary cells. *Am. J. Physiol.* **1997**, *272*, E405–E414. [CrossRef]

25. Barthel, L.; Reetz, O.; Strauss, U. Use dependent attenuation of rat HCN1-mediated I_h in Intact HEK293 Cells. *Cell Physiol. Biochem.* **2016**, *38*, 2079–2093. [CrossRef]

26. Fürst, O.; D'Avanzo, N. Isoform dependent regulation of human HCN channels by cholesterol. *Sci. Rep.* **2015**, *5*, 14270. [CrossRef]

27. Männikkö, R.; Pandey, S.; Larsson, H.P.; Elinder, F. Hysteresis in the voltage dependence of HCN channels: Conversion between two modes affects pacemaker properties. *J. Gen. Physiol.* **2005**, *125*, 305–326. [CrossRef]

28. Cabral, P.H.; de Morais Campos, R.; Fonteles, M.C.; Santos, C.F.; Leal Cardoso, J.H.; do Nascimento, N.R. Effects of the essential oil of Croton zehntneri and its major components, anethole and estragole, on the rat corpora cavernosa. *Life Sci.* **2014**, *112*, 74–81. [CrossRef]

29. Berger, F.; Borchard, U.; Hafner, D.; Kammer, T.; Weis, T. Inhibition of potassium outward currents and pacemaker current in sheep cardiac Purkinje fibres by the verapamil derivative YS 035. *Naunyn. Schmiedebergs Arch. Pharmacol.* **1991**, *344*, 653–661. [CrossRef]

30. Dini, L.; Del Lungo, M.; Resta, F.; Melchiorre, M.; Spinelli, V.; Di Cesare Mannelli, L.; Ghelardini, C.; Laurino, A.; Sartiani, L.; Coppini, R.; et al. Selective blockade of HCN1/HCN2 channels as a potential pharmacological strategy against pain. *Front. Pharmacol.* **2018**, *9*, 1252. [CrossRef]

31. Resta, F.; Micheli, L.; Laurino, A.; Spinelli, V.; Mello, T.; Sartiani, L.; Di Cesare Mannelli, L.; Cerbai, E.; Ghelardini, C.; Romanelli, M.N.; et al. Selective HCN1 block as a strategy to control oxaliplatin-induced neuropathy. *Neuropharmacology* **2018**, *131*, 403–413. [CrossRef] [PubMed]

32. Wu, S.N.; Yang, W.H.; Yeh, C.C.; Huang, H.C. The inhibition by di(2-ethylhexyl)-phthalate of *erg*-mediated K^+ current in pituitary tumor (GH_3) cells. *Arch. Toxicol.* **2012**, *86*, 713–723. [CrossRef] [PubMed]

33. Albertson, A.J.; Bohannon, A.S.; Hablitz, J.J. HCN channel modulation of synaptic integration in GABAergic interneurons in malformed rat neocortex. *Front. Cell Neurosci.* **2017**, *11*, 109. [CrossRef] [PubMed]

34. Datunashvili, M.; Chaudhary, R.; Zobeiri, M.; Luttjohann, A.; Mergia, E.; Baumann, A.; Balfanz, S.; Budde, B.; van Luijtelaar, G.; Pape, H.C.; et al. Modulation of hyperpolarization-activated inward current and thalamic activity modes by different cyclic nucleotides. *Front. Cell Neurosci.* **2018**, *12*, 369. [CrossRef]

35. Kuo, P.C.; Yang, C.J.; Lee, Y.C.; Chen, P.C.; Liu, Y.C.; Wu, S.N. The comprehensive electrophysiological study of curcuminoids on delayed-rectifier K^+ currents in insulin-secreting cells. *Eur. J. Pharmacol.* **2018**, *819*, 233–241. [CrossRef]

36. Zhang, Y.; Liu, Y.; Qu, J.; Hardy, A.; Zhang, N.; Diao, J.; Strijbos, P.J.; Tsushima, R.; Robinson, R.B.; Gaisano, H.Y.; et al. Functional characterization of hyperpolarization-activated cyclic nucleotide-gated channels in rat pancreatic beta cells. *J. Endocrinol.* **2009**, *203*, 45–53. [CrossRef]

37. Skelin, M.; Rupnik, M.; Cencic, A. Pancreatic beta cell lines and their applications in diabetes mellitus research. *ALTEX* **2010**, *27*, 105–113. [CrossRef]

38. Lainez, S.; Tsantoulas, C.; Biel, M.; McNaughton, P.A. HCN3 ion channels: Roles in sensory neuronal excitability and pain. *J. Physiol.* **2019**, *597*, 4661–4675. [CrossRef]

39. Zhao, W.; Liang, P.; Liu, J.; Li, H.; Liao, D.; Chen, X.; Li, Q.; Zhou, C. Capsazepine prolongation of the duration of lidocaine block of sensory transmission in mice may be mediated by modulation of HCN channel currents. *PeerJ* **2019**, *7*, e7111. [CrossRef]

40. Djouhri, L.; Smith, T.; Ahmeda, A.; Alotaibi, M.; Weng, X. Hyperpolarization-activated cyclic nucleotide-gated channels contribute to spontaneous activity in L4 C-fiber nociceptors, but not Aβ-non-nociceptors, after axotomy of L5-spinal nerve in the rat in vivo. *Pain* **2018**, *159*, 1392–1402. [CrossRef]

41. Kuo, P.C.; Shen, Y.C.; Yang, M.L.; Wang, S.H.; Thang, T.D.; Dung, N.X.; Chiang, P.C.; Lee, K.H.; Lee, E.J.; Wu, T.S. Crotonkinins A and B and related diterpenoids from Croton tonkinensis as anti-inflammatory and antitumor agents. *J. Nat. Prod.* **2007**, *70*, 1906–1909. [CrossRef] [PubMed]

42. Hsiao, H.T.; Lee, Y.C.; Liu, Y.C.; Kuo, P.C.; Wu, S.N. Differential suppression of delayed-rectifier and inwardly rectifier K^+ currents by a group of ent-kaurane-type diterpenoids from Croton tonkinensis, in microglial cells. *Eur. J. Pharmacol.* **2019**, *856*, 172414. [CrossRef]

43. Wu, S.N.; Chern, J.H.; Shen, S.; Chen, H.H.; Hsu, Y.T.; Lee, C.C.; Chan, M.H.; Lai, M.C.; Shie, F.S. Stimulatory actions of a novel thiourea derivative on large-conductance, calcium-activated potassium channels. *J. Cell Physiol.* **2017**, *232*, 3409–3421. [CrossRef] [PubMed]

44. Gadagkar, S.R.; Call, G.B. Computational tools for fitting the Hill equation to dose-response curves. *J. Pharmacol. Toxicol. Methods* **2015**, *71*, 68–76. [CrossRef] [PubMed]